Supplementary Information

Synthesis and supramolecular liquid crystalline structure modulation of side-chain polynorbornenes with asymmetrical substituent mesogenic groups

Yuanyang Tu,[a]   Yijin Wu,[a] Jiwei Pei,[a] Wentao Qu,[b] Huanjun Lu,[a] Feng Liu,*[b] and Xiao-Fang Chen*[a]

[a]Suzhou Key Laboratory of Macromolecular Design and Precision Synthesis, Jiangsu Key Laboratory of Advanced Functional Polymer Design and Application, State and Local Joint Engineering Laboratory for Novel Functional Polymeric Materials, College of Chemistry, Chemical Engineering and Materials Science, Soochow University, Suzhou 215123, P. R. China

[b]State Key Laboratory for Mechanical Behavior of Materials, Shaanxi International Research Center for Soft Matter, School of Materials Science & Engineering, Xi'an Jiaotong University, Xi'an 710049, P. R. China

E-mail: xfchen75@suda.edu.cn, feng.liu@mail.xjtu.edu.cn

Materials

4'-Hydroxy-biphenyl-4-carboxylic acid (99%), 1-Bromododecane (97%), Lithium aluminum hydride (95%), Potassium iodide (99%), Methyl 2-hydroxybenzoate (99%), Methyl 3-hydroxybenzoate (99%), Methyl 2,3-dihydroxybenzoate (98%), 1-[3-(Dimethylamino) propyl]-propyl]-3-ethylcarbodiimide hydrochloride (EDC·HCl, 99%), 4-(Dimethylamino) pyridine (DMAP, 99%), and Grubbs catalyst (third generation) were purchased from Sigma Aldrich. Dichloromethane (CH_2Cl_2) (AR, Sinopharm) and Trichloromethane ($CHCl_3$) (AR, Sinopharm) were distilled by refluxing over CaH_2 prior to use. Tetrahydrofuran (THF) (AR, Sinopharm) was heated under reflux over sodium for at least 8 h and distilled before use. N-(2-hydroxyethyl)-*cis*-5-norbornene-*exo*-2,3-dicarboximide, N-(6-hydroxyhexyl)-*cis*-nor-bornene-*exo*-2,3-dicarboximide, and N-(8-hydroxyoctyl)-*cis*-5-norbornene-*exo*-2,3-dicar-boximide were prepared according to literature procedure. All other reagents and solvents were obtained from commercial sources and used without further purification.

Measurements

TGA. The thermal stability of all the polymers was measured by Thermal Gravimetric Analysis (TGA) on a TGA Q500 (TA) instrument at a heating rate of 10 °C·min^{-1} from ambient temperature to 800 °C under a nitrogen atmosphere.

POM. Polarized optical microscopy (POM) observations of the liquid crystalline textures of the polymers were performed on an Olympus BX51-P microscope equipped with a Linkam THMS 600 hot stage. Samples were made by sandwiching the dried polymer powder between a glass slide and a cover glass. Heating these samples to their isotropic temperature and being annealed 10 min at isotropic temperature, the samples were cooled to room temperature at a rate of 1 °C·min^{-1}.

AFM. Surface morphologies of thin films were recorded by atomic force microscopy (AFM) using Bruker (Digital Instruments) Multi-Mode AFM under tapping mode. Samples are deposited on piranha cleaned silicon substrates by spin casting 10 mg·ml^{-1} polymer solution (2000 rpm) to obtain thin film samples approximately 100 nm thickness. The samples were annealed under vacuum for 24 h and slowly cooled to room temperature. The AFM images were recorded using tapping mode with a scan rate of 0.97 Hz, wherein the cantilever force was controlled to be large enough to explore the surface features, yet small enough to avoid the sample damage.

Electron density reconstruction. Two-dimensional electron density maps could be reconstructed on the basis of the general formula:

$$\rho(xy) = \sum_{hk} F(hk) exp[i2\pi(hx + ky)]$$

Here *F*(*hk*) is the structure factor of a diffraction peak with index (*hk*). The experimentally observed diffraction intensity

$$I(hk) = K \cdot F(hk) \cdot F^*(hk) = K \cdot |F(hk)|^2$$

Here K is a constant related to the sample volume, incident beam intensity etc. In this paper

we are only interested in the relative electron densities, hence this constant is simply taken to be 1. Thus the electron density:

$$\rho(xy) = \sum_{hk} sqrt[I(hk)]exp\left[i2\pi(hx + ky) + \emptyset_{hk}\right]$$

Here ϕ_{hk} is the phase angle of the *hk* Bragg reflection.

As the observed diffraction intensity $I(hk)$ is only related to the amplitude of the structure factor $|F(hk)|$, the information about the phase of $F(hk)$, ϕ_{hk}, cannot be determined directly from experiment. However, the problem is significantly simplified with most space group symmetries, where the phase angle ϕ_{hk} of a given (*hk*) reflection has limited choices. In this work, the self-assembly structure has a *p*2 symmetry, which is centrosymmetric. Thus the phase angle ϕ_{hk} is limited to 0 or π.
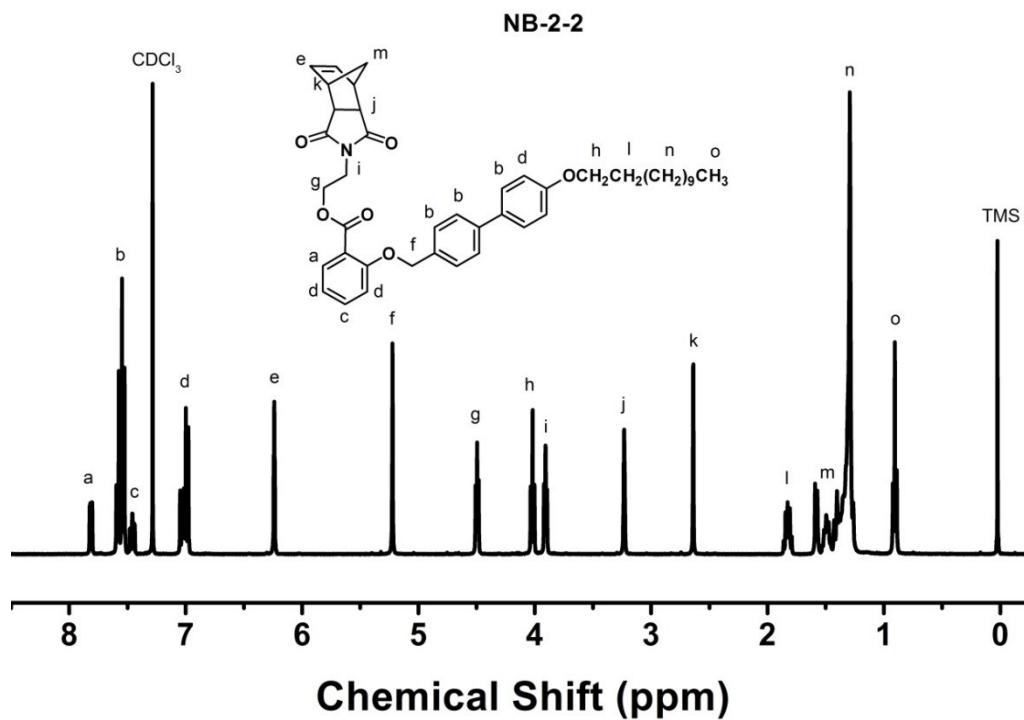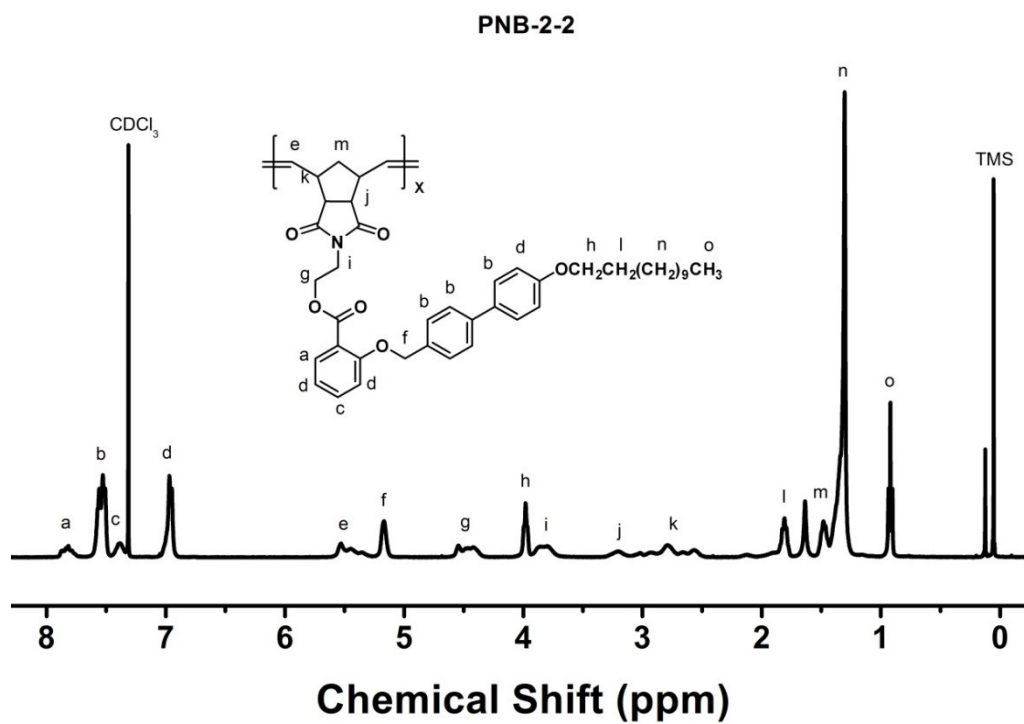
Fig. S1 ^{1}H NMR spectra of NB-2-2 (a) and PNB-2-2 (b) in CDCl$_3$.
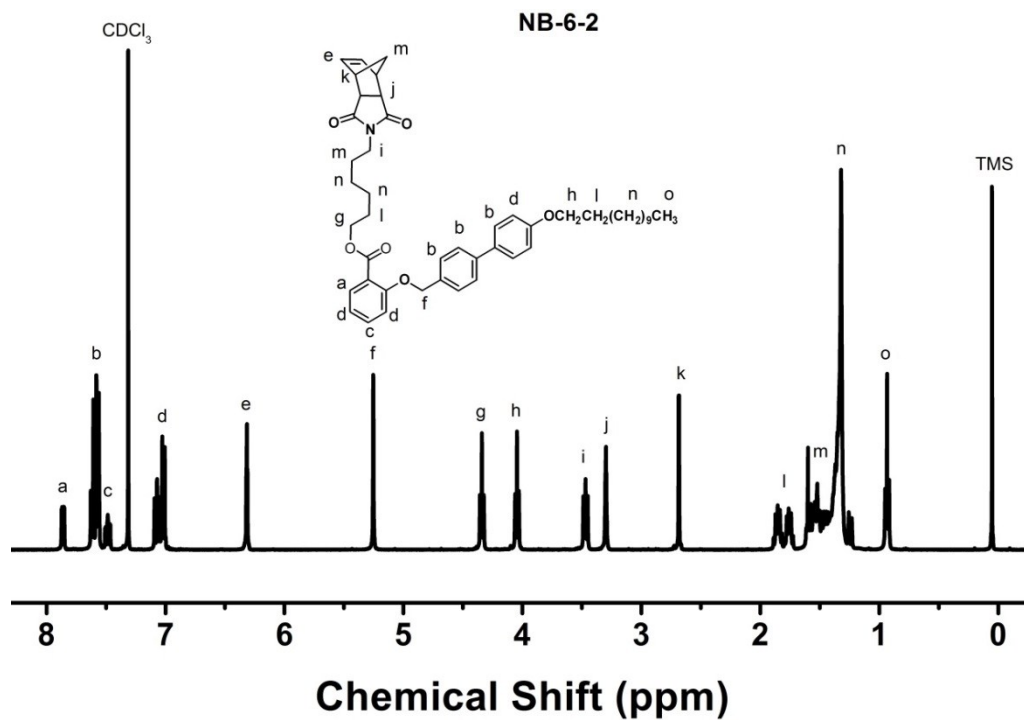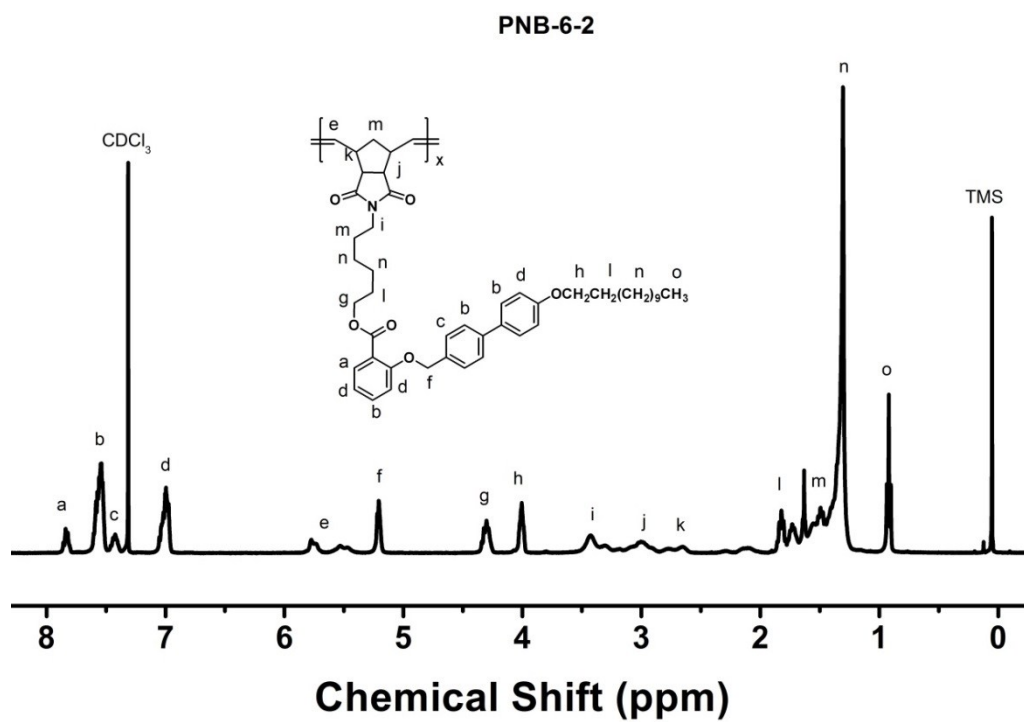
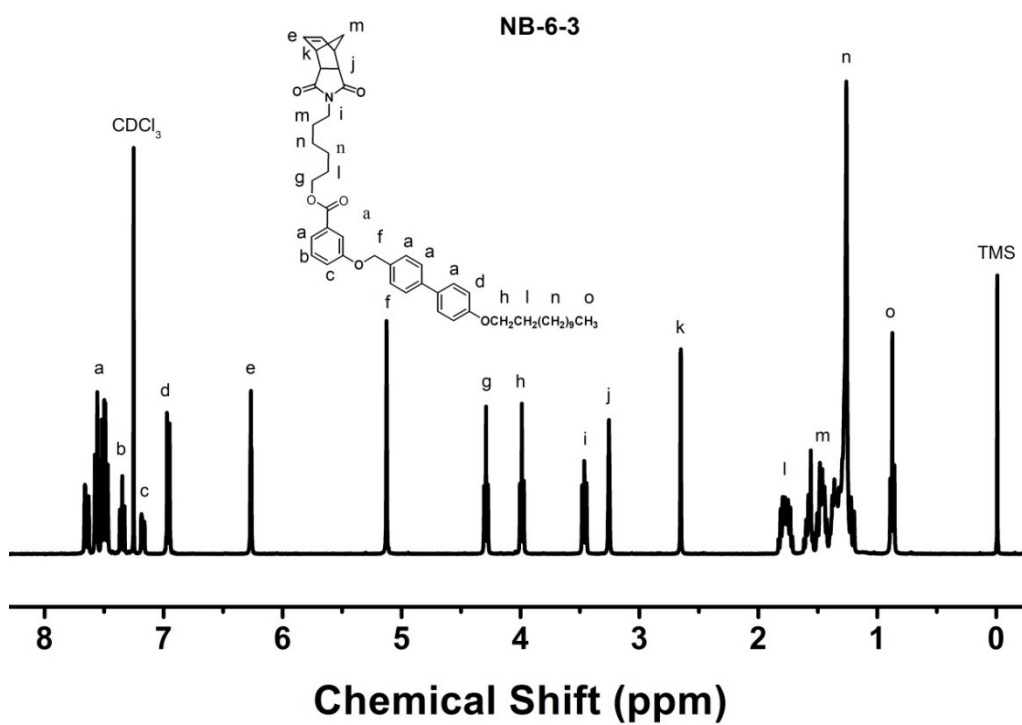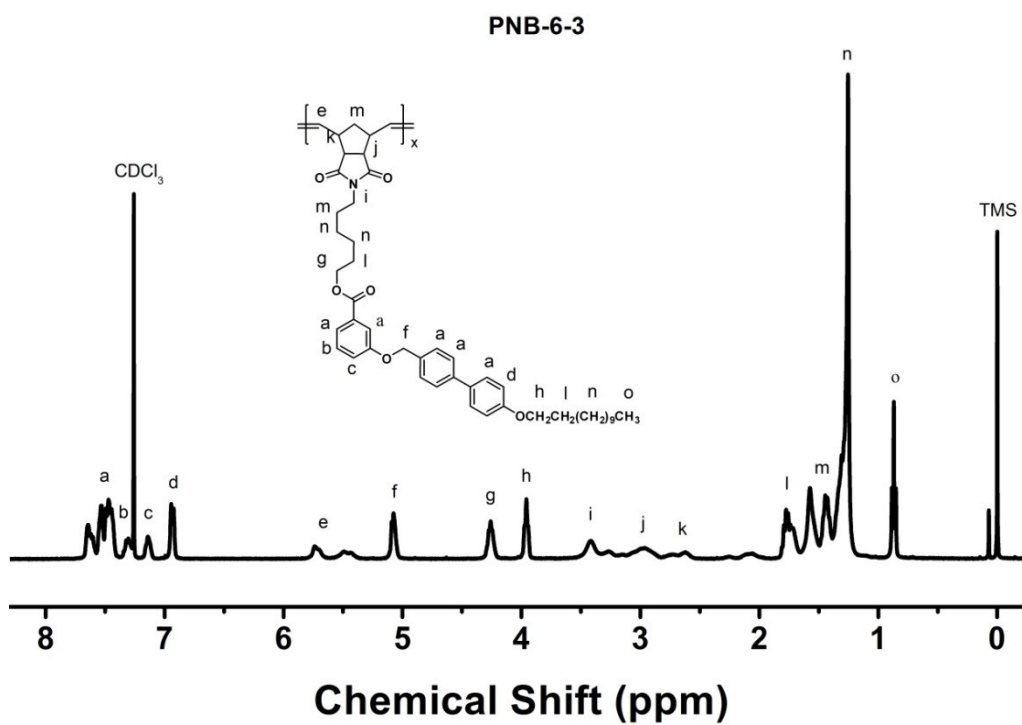**Fig. S2** ^{1}H NMR spectra of NB-6-2 (a) and PNB-6-2 (b) in CDCl$_3$.
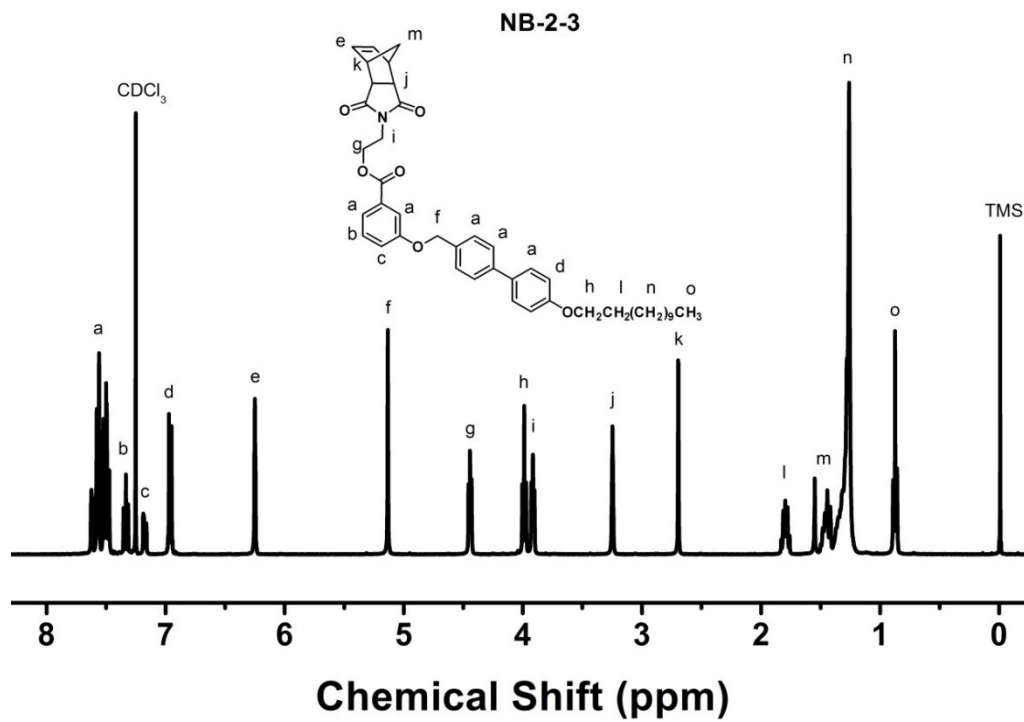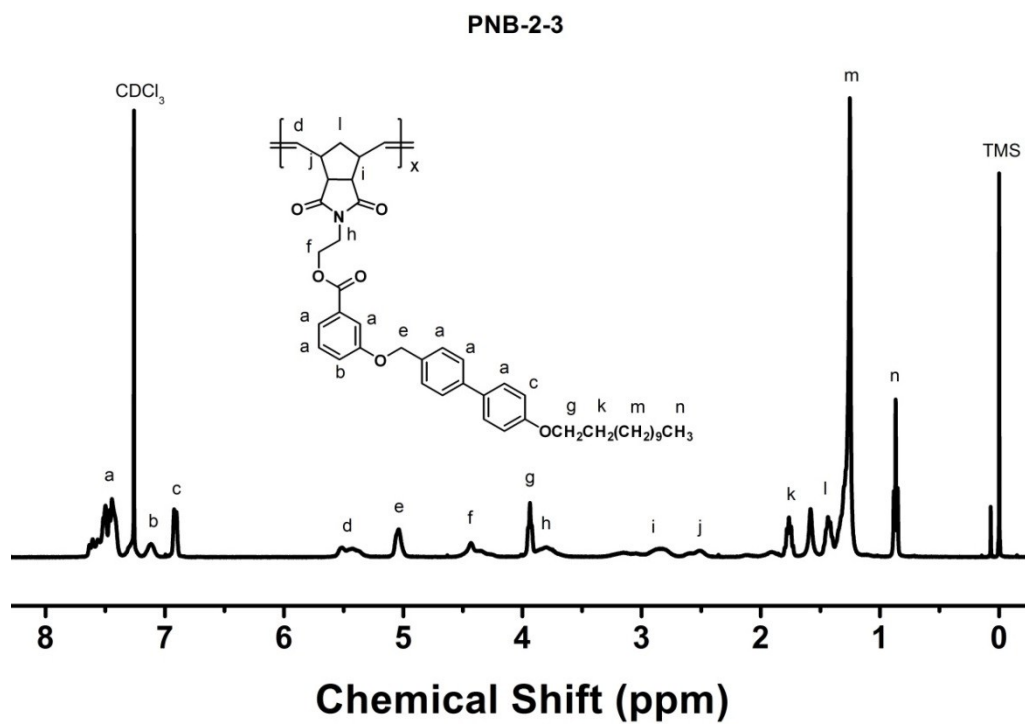
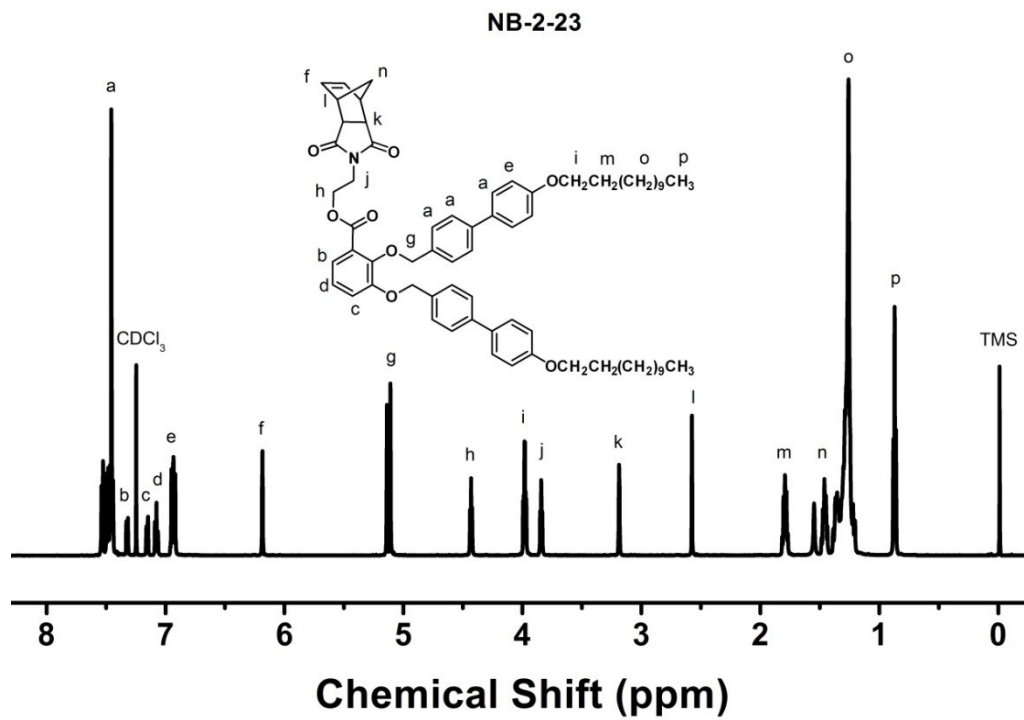**Fig. S3** ^{1}H NMR spectra of NB-2-3 (a) and PNB-2-3 (b) in CDCl$_3$.

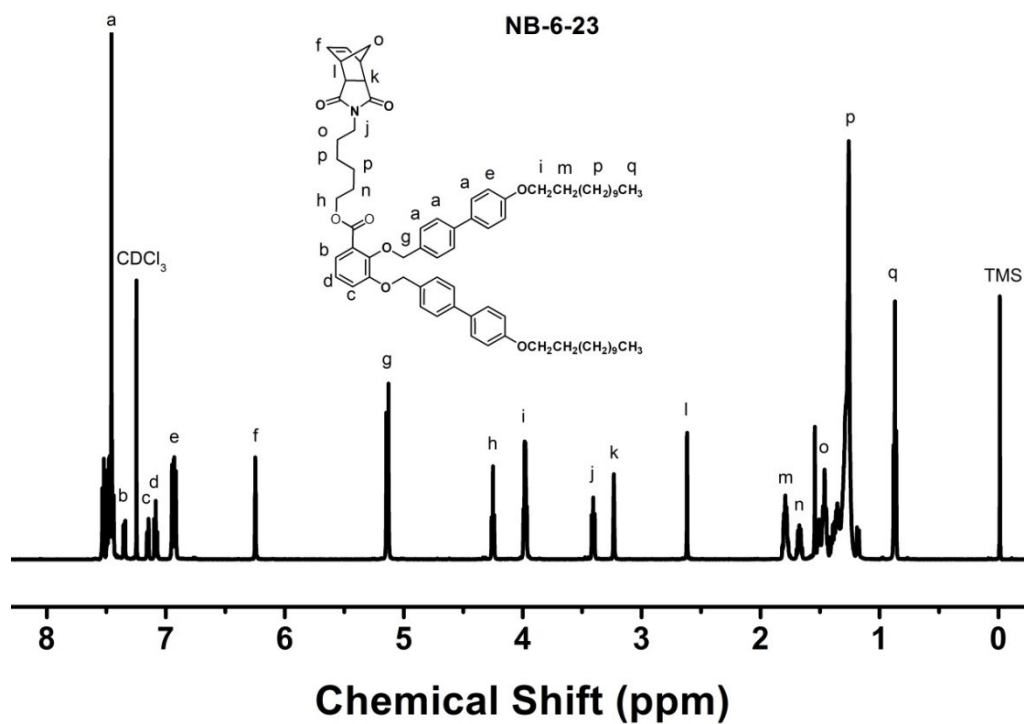**Fig. S4** ^{1}H NMR spectra of NB-6-3 (a) and PNB-6-3 (b) in CDCl[3].
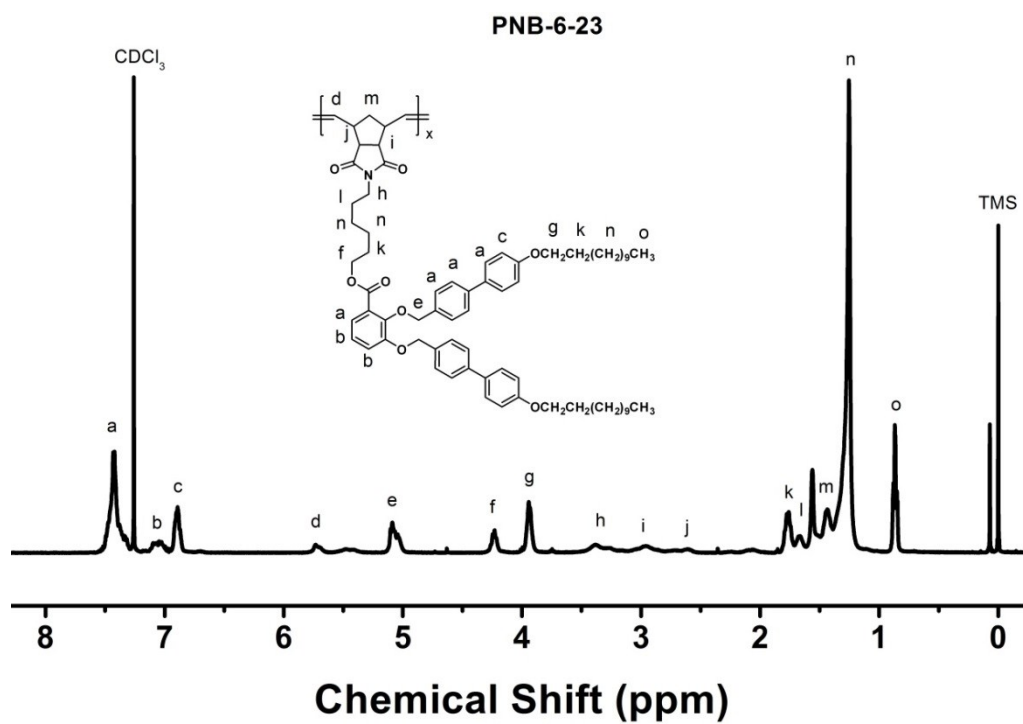
NB-2-23

(a)
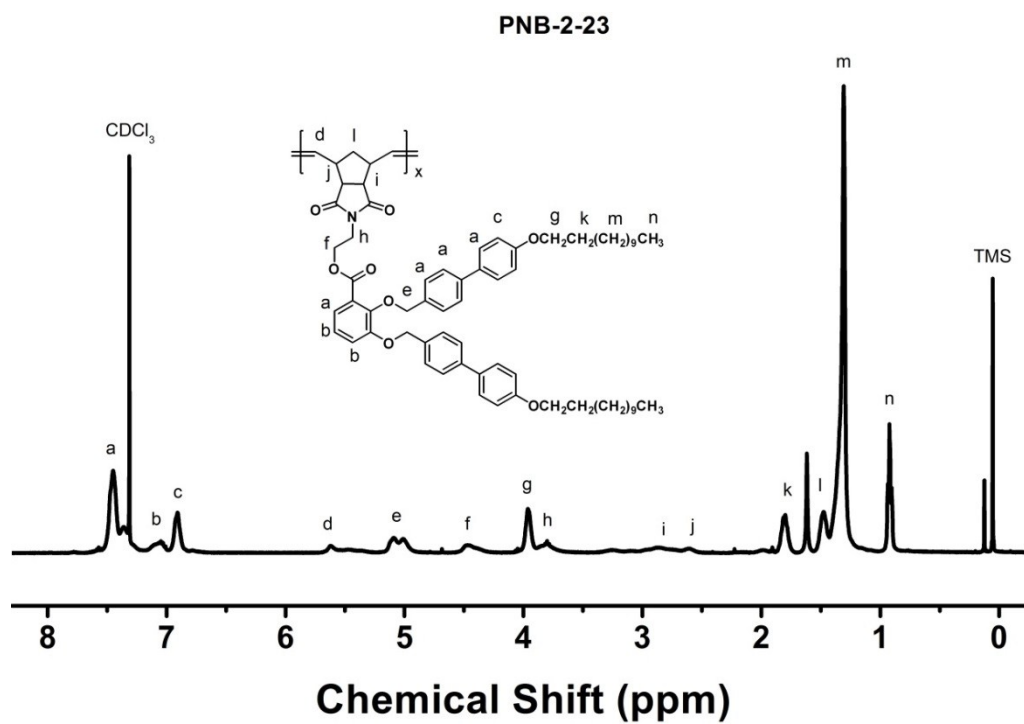
PNB-2-23

(b)

Figure S5. ^{1}H NMR spectra of NB-2-23 (a) and PNB-2-23 (b) in CDCl$_3$.

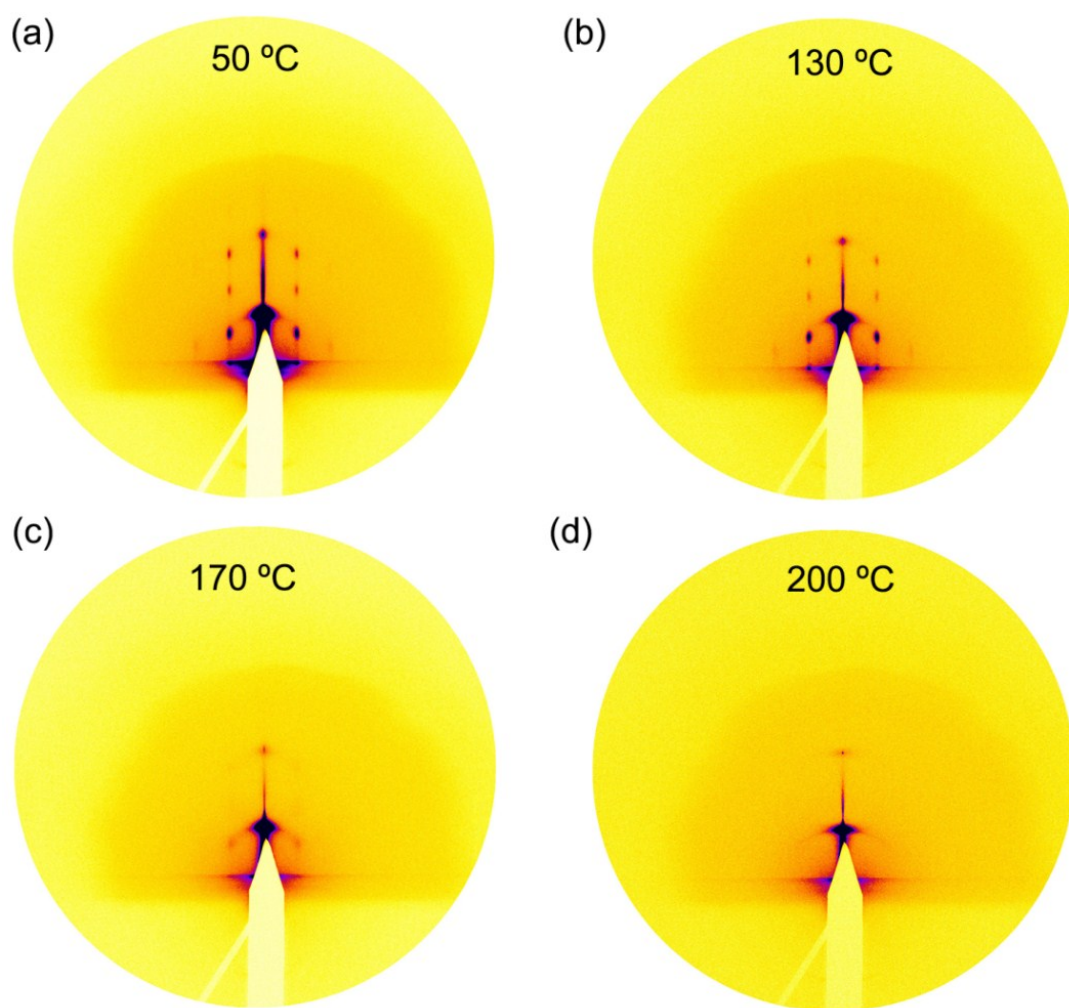**Fig. S6** ^{1}H NMR spectra of NB-6-23 (a) and PNB-6-23 (b) in CDCl$_3$.

Fig. S7 Temperature-dependent GISAXS profiles of PNB-2-23 recorded at (a) 50 °C; (b) 130 °C; (c) 170 °C; (d) 200 °C.
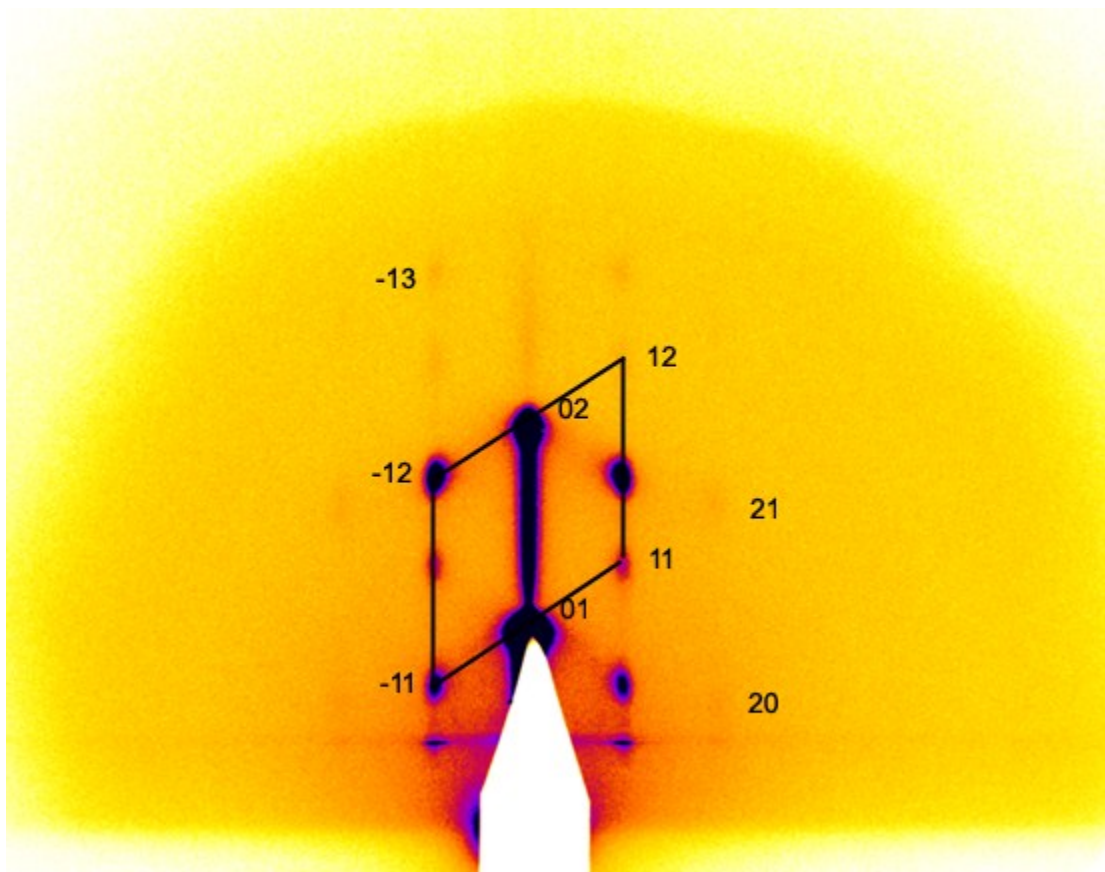
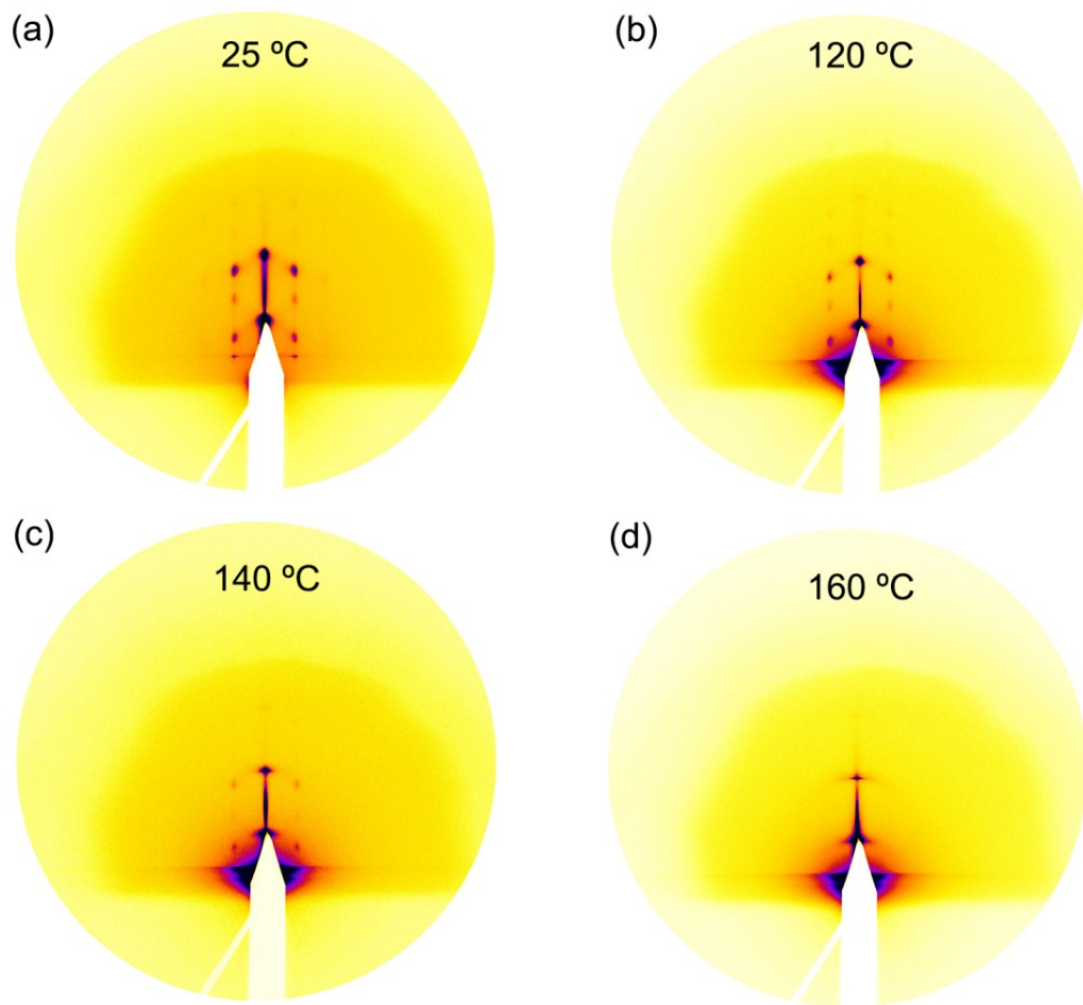**Fig. S8** GISAXS profiles of PNB-6-23 recorded at room temperature.

Fig. S9 Temperature-dependent GISAXS profiles of PNB-8-23 recorded at (a) 25 ^{o}C; (b) 120 ^{o}C; (c) 140 ^{o}C; (d) 160 ^{o}C.
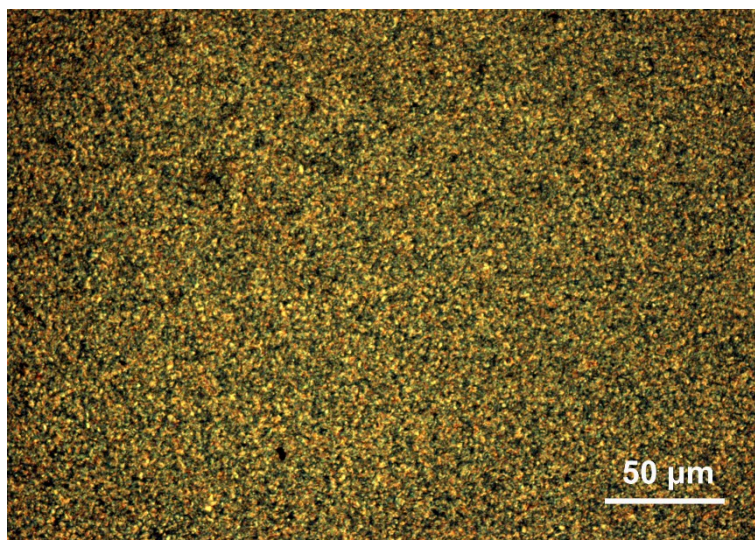
Fig. S10 POM picture of PNB-6-23 taken at 170 °C when cooling the sample from isotropic state at a rate of 1 °C·min^{-1}.
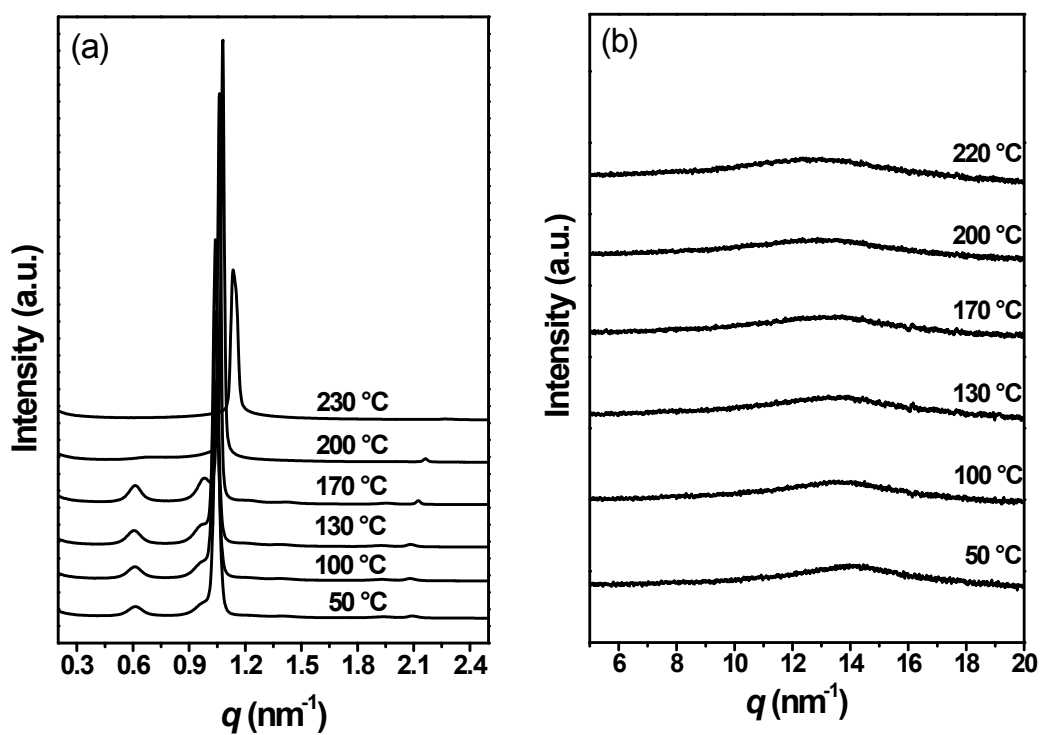

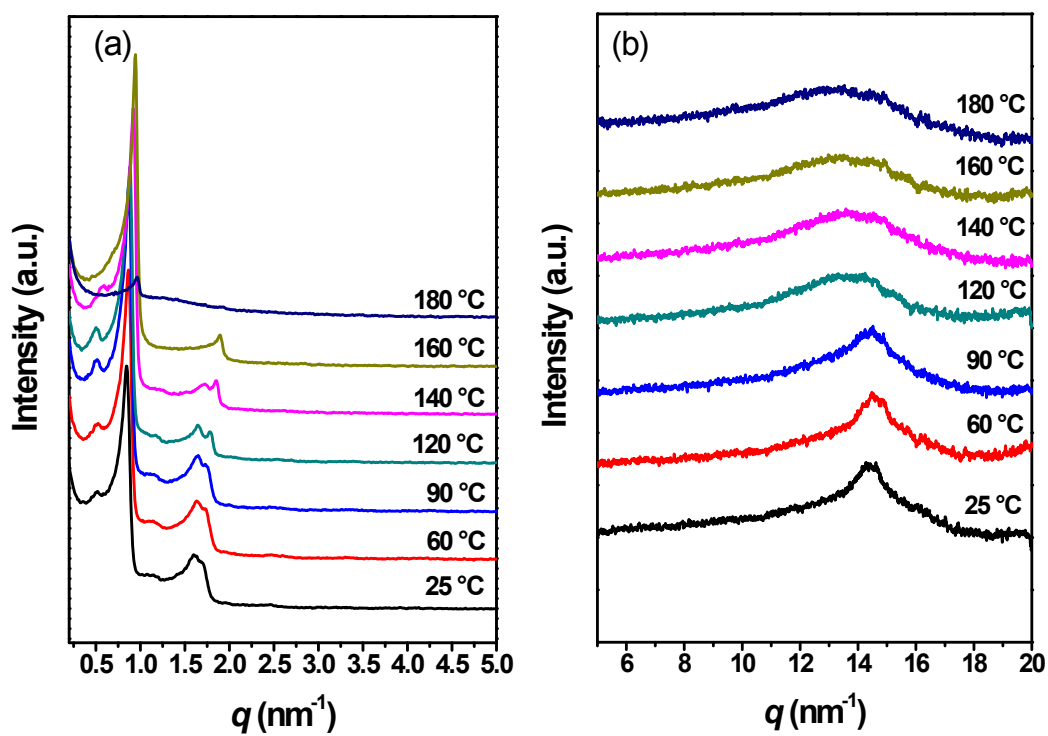**Fig. S11** Temperature-dependent SAXS (a) and WAXS (b) profiles of PNB-2-23.

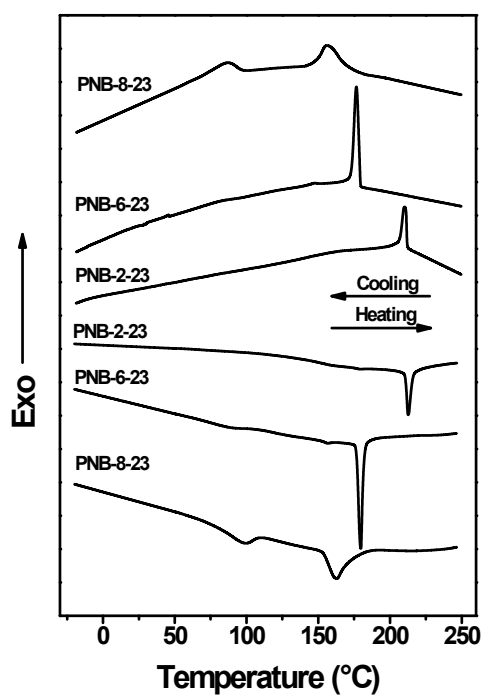**Fig S12** Temperature-dependent SAXS (a) and WAXS (b) profiles of PNB-8-23.

Fig. S13 DSC curves of PNBs during the first cooling and the second heating cycle at a rate of 10 °C·min^{-1} under a N$_2$ atmosphere.

Table S1 Experimental and calculated *d*-spacings, relative integrated intensities and phases used in electron density reconstruction for the observed hk0 SAXS reflections of the oblique phase of PNB-6-23 at 150 °C. All intensity values are Lorentz and multiplicity corrected.

(*hk*)	$d_{obs.}$ –spacing (nm)	$d_{cal.}$ –spacing (nm)	*intensity*	*phase*
(10)	11.44	11.42	14.48	π
(01)	6.55	6.54	100.00	π
(20)	5.68	5.71	1.22	π
(11)	4.87	4.86	0.88	π
(12)	3.55	3.61	2.48	π
(02)	3.27	3.27	2.94	/
a = 12.60 nm, *b* = 7.22 nm, γ = 115°				